MgO codoping-induced change in the site distribution of Cr^{3+} ions in $LiNbO_3$

J. Díaz-Caro,* J. García-Solé, D. Bravo, J. A. Sanz-García, F. J. López, and F. Jaque
Departamento de Física de Materiales (C-IV), Universidad Autónoma de Madrid, Cantoblanco, Madrid 28049, Spain
(Received 9 February 1996; revised manuscript received 20 May 1996)

Optical absorption and electron paramagnetic resonance (EPR) have been applied in parallel to investigate $LiNbO_3$:Cr[0.1%] and $LiNbO_3$:Cr[0.1%], Mg[X%] crystals ($X=2$, 4, 5, 5.5, and 6). From the data obtained, it has been concluded that Cr^{3+} ions occupy both Li^+ and Nb^{5+} sites. In Mg undoped crystals the optical absorption and EPR spectra are attributed to Cr^{3+} ions in Li^+ site. In crystals with Mg doping levels greater than 4.6 mol % both Li^+ and Nb^{5+} sites are occupied, their relative concentration being governed by the Mg^{2+} content. The double occupancy affects the overall absorption spectrum, giving rise to reproducible color changes in the crystal. Finally, the threshold found for the occupation of Cr^{3+} ions in Nb^{5+} sites is discussed considering the different models related to the nonstoichiometry of $LiNbO_3$. [S0163-1829(96)03241-9]

I. INTRODUCTION

Since the report of cw laser action in $LiNbO_3$:MgO,Nd,[1] interest in the research of optically active ions, other than Nd^{3+}, has been promoted. Particular interest exists in Cr^{3+} ions because of the possibility of realizing tunable lasers based on this nonlinear host crystal, as a result of the broadband spectral characteristics of this ion.[2]

The Cr^{3+} ion in $LiNbO_3$ has been investigated by optical,[3–6] electron paramagnetic resonance[7–10] (EPR), and electron nuclear double resonance[11] (ENDOR) spectroscopies. In spite of the fact that a full understanding of the spectroscopy of this ion in $LiNbO_3$ is still lacking, some relevant conclusions have been established.

(i) By a systematic analysis of the R-line emission spectral range, the formation of nonequivalent Cr^{3+} centers (Cr^{3+} ions in different local symmetries) was ascertained.[4–6] However, in the EPR spectrum only one axial Cr^{3+} spectrum was detected, and tentatively associated with Cr^{3+} ions in Li^+ sites (Cr^{3+}_{Li} center).[11]

(ii) Both optical and EPR spectra are substantially modified by codoping with 5% or more of MgO, which becomes necessary in laser applications in order to reduce the photorefractive damage.[12] This codoping gives rise to new R lines (additional Cr^{3+} centers) and also modifies the overall absorption spectrum, producing a different color in the crystal.[5] Changes are also manifested in the EPR spectrum through the appearance of new isotropic features in the spectrum, which have been associated with Cr^{3+} ions occupying Nb^{5+} sites (Cr^{3+}_{Nb} center).[10,11]

Irrespective of the nature of the Cr^{3+} centers, it seems to be clear that MgO codoping affects the distribution of the Cr^{3+} ions among the available structural sites in $LiNbO_3$.

Recent experiments by Rutherford backscattering spectrometry (RBS) and channeling have proved that both rare earth and transition metal ions in $LiNbO_3$ lie in Li^+ octahedral sites.[13] In spite of the fact that Cr^{3+} ions are very light and cannot be detected by RBS in $LiNbO_3$, it is expected that they also lie in Li^+ sites.

In this work the optical absorption spectrum of Cr^{3+} in $LiNbO_3$ has been systematically investigated as a function of MgO codoping. EPR spectroscopy has also been used in parallel, to probe the site occupied by the Cr^{3+} ions. Experimental results clearly reveal that a certain fraction of Cr^{3+} ions is displaced from Li^+ to Nb^{5+} sites if the MgO codopant concentration is greater than 4.6%. Above this Mg threshold value, the Cr^{3+}_{Nb} content is linearly dependent on the codopant concentration. These changes in the distribution ratio of Cr^{3+}_{Li} and Cr^{3+}_{Nb} centers account for the color change observed in the crystals by MgO codoping.

II. EXPERIMENTAL DETAILS

Congruent $LiNbO_3$:Cr and $LiNbO_3$:Cr,Mg crystals were grown in air by the Czochralski method from grade-I Johnson-Mathey powder pulling the seed along ferroelectric c axis. The singly and doubly doped samples had a [Cr]/[Nb] concentration ratio of 0.1% in the melt. Five doubly doped crystals were grown with [Mg]/[Nb] concentration ratios of 2%, 4%, 5%, 5.5%, and 6% from congruent melts ([Li]/[Nb]=0.945).

The [Cr]/[Nb] ratio in the crystal was determined by total-reflection x-ray fluorescence[14] (TRXRF) with a relative error lower than 5%. Cr concentration values between 0.21% and 0.27% were found. This higher content of chromium in the crystal with respect to the chromium concentration in the melt is in accordance with the Cr effective distribution coefficient in $LiNbO_3$ ($k_{eff}=2.0$),[15] although this parameter is highly dependent on particular growth conditions.[16]

For optical absorption measurements, plate samples of $LiNbO_3$:Cr and $LiNbO_3$:Cr,Mg were cut perpendicular to the c axis (c cut) with 4 mm thickness and their faces were carefully polished. Thus, spectra were all taken on the α configuration (light beam propagating along the c axis, $\mathbf{E}\perp c$). The sample without magnesium has been labeled as $S0$ and the codoped crystals as $S2$, $S4$, $S5$, $S55$, and $S6$, depending, respectively, on their Mg concentration in the melt (0%, 2%, 4%, 5%, 5.5%, and 6%). The absorption spectra were carried out with a Hitachi U-3501 spectrophotometer at room temperature.

For EPR measurements, all samples were prepared with similar shape and dimensions (10 mm×4 mm×1 mm), being the crystallographic c axis along the 4 mm side. The

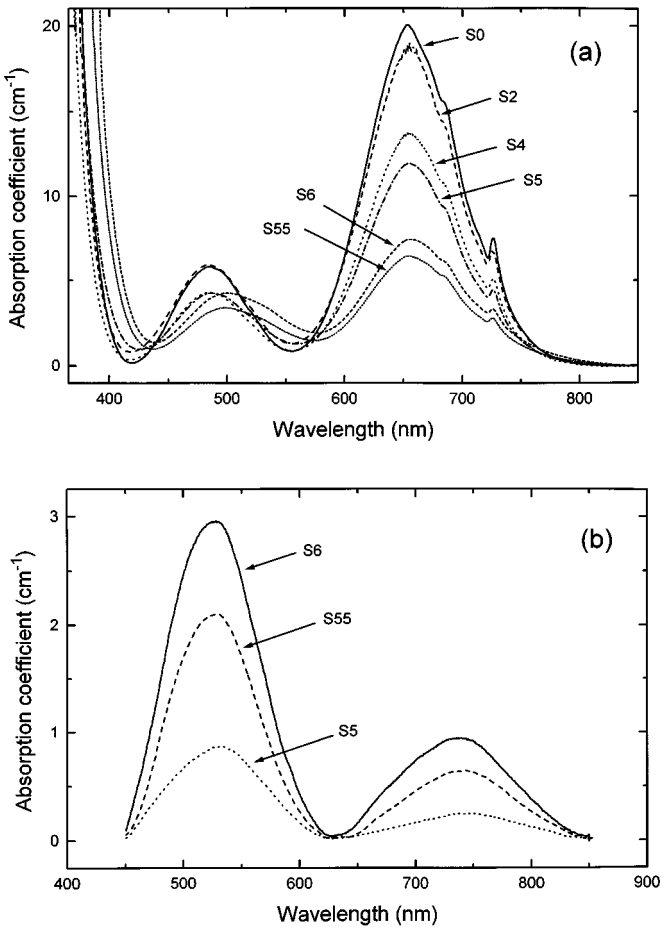

FIG. 1. (a) Absorption spectra of the $LiNbO_3$:Cr[0.1%] and $LiNbO_3$:Cr[0.1%],Mg[X%] crystals ($X=2$, 4, 5, 5.5, and 6), labeled, respectively, as $S0$, $S2$, $S4$, $S5$, $S55$, and $S6$, measured at room temperature. (b) Deconvolutioned absorption spectra of the $S5$, $S55$, and $S6$ samples on the basis of the spectrum of the $S0$ crystal.

choice of similar sample shape and volume is important in order to obtain approximately the same EPR cavity filling factor for all samples.[17] In this way, measurements of relative line intensities can be carried out reliably.

The EPR spectra have been obtained at room temperature by means of a Bruker ESP 300 E spectrometer working in the X band, with a field modulation of 100 kHz. The samples were mounted on a homemade two-axis goniometer, so that they could be rotated in two perpendicular planes.

III. EXPERIMENTAL RESULTS AND DISCUSSION

Figure 1(a) shows the absorption spectra of chromium doped $LiNbO_3$ crystal ($S0$) and chromium-magnesium oxide codoped $LiNbO_3$ crystals ($S2$, $S4$, $S5$, $S55$, and $S6$) in the spectral range 360–850 nm. The absorption coefficients have been normalized to account for the small deviation in the total chromium concentration in the crystals measured by TRXRF.

The features of optically active Cr^{3+} ions appear in all spectra. These are dominated by two broadbands centered at 487 and 654 nm, due, respectively, to the spin-allowed $^4A_2\rightarrow{}^4T_1$ and $^4A_2\rightarrow{}^4T_2$ vibronic transitions, and by a narrow band located at 727 nm. At low temperature this 727 nm absorption band splits in three narrow lines at 723.9, 726, and 730.3 nm. The nature of these last absorption transitions is still not well known. In fact, they have been attributed to the spin-forbidden $^4A_2\rightarrow{}^2E$ transitions[3,5,6,18] (R lines) as well as to hot-phonon sidebands of the $^4A_2\rightarrow{}^4T_2$ transition.[4]

As can be seen from Fig. 1(a), the area under the optical absorption spectrum decreases when the magnesium content in the crystal increases. The absorption coefficient of the $^4A_2\rightarrow{}^4T_2$ broadband transition drops to 30% of the 0% Mg crystal when the Mg concentration reaches 6%. It is important to emphasize that, in addition to this descent in the optical absorption, the peak position of the high-energy broadband $^4A_2\rightarrow{}^4T_2$ appears displaced to lower energy for crystals with a Mg concentration greater than 4%. Moreover, the $^4A_2\rightarrow{}^4T_2$ band seems to be weakly broadened towards the infrared side of the spectrum.

The optical dip observed between the two absorption broadbands produces an apparent optical window. For the Mg undoped $LiNbO_3$:Cr sample ($S0$) the position of the window appears centered at about 555 nm, and it is responsible for the green color. In Mg-doped $LiNbO_3$:Cr crystals this optical dip is displaced to higher wavelengths, producing a color change to pink. The observed color change could also be affected by the variation in the absorption coefficient in the ultraviolet range. This aspect will be discussed later.

The above-mentioned absorption changes suggest the formation of new bands in the absorption spectrum of $LiNbO_3$:Cr when Mg ions are incorporated into the crystal. The optical absorption spectra shown in Fig. 1(b) are the result of deconvoluting the spectra of $S5$, $S55$, and $S6$ samples, obtained after subtraction of the unperturbed $S0$ spectrum appropriately scaled. Two new weak absorption bands centered at 530 and 745 nm are now clearly observed. No new bands were detected in the deconvoluted spectra of $S2$ and $S4$ crystals. Similar absorption bands were previously reported in $LiNbO_3$:Cr,Mg crystals and assigned to the $^4A_2\rightarrow{}^4T_1$ and $^4A_2\rightarrow{}^4T_2$ vibronic transitions of an additional Cr^{3+} center in a lower crystal field.[5]

The evolution of the integrated absorption broadbands centered at 654 and 530 nm as a function of Mg concentration is shown in Fig. 2. It is important to point out that while the total chromium concentration keeps constant with the Mg content (upper part of Fig. 2), the integrated absorption area of the 654 nm band presents a nonlinear decreasing that reaches 30% for the $S6$ crystal (6% Mg doping level) with respect to the $S0$ sample. The same trend with the Mg content has been found for the 487 nm broadband. However, it should be noted that the new pair of broadbands (the 745 nm band displays the same behavior as the 530 nm one) is only detected for Mg concentration higher than 4%, showing thereafter a well-defined linear increasing behavior as the Mg concentration increases. Extrapolating this linear fitting, an apparent threshold is observed for the appearance of these new bands at a Mg concentration of 4.6%. From Fig. 2 it is also inferred that the Cr^{3+} optical absorption decreases in the MgO doping range from 0 to 4.6%, while the new bands associated with the Cr^{3+} ions in a lower crystal field are not yet formed. Therefore, since the total chromium concentration remains constant and is independent of the MgO content, these data strongly suggest that Cr ions with different

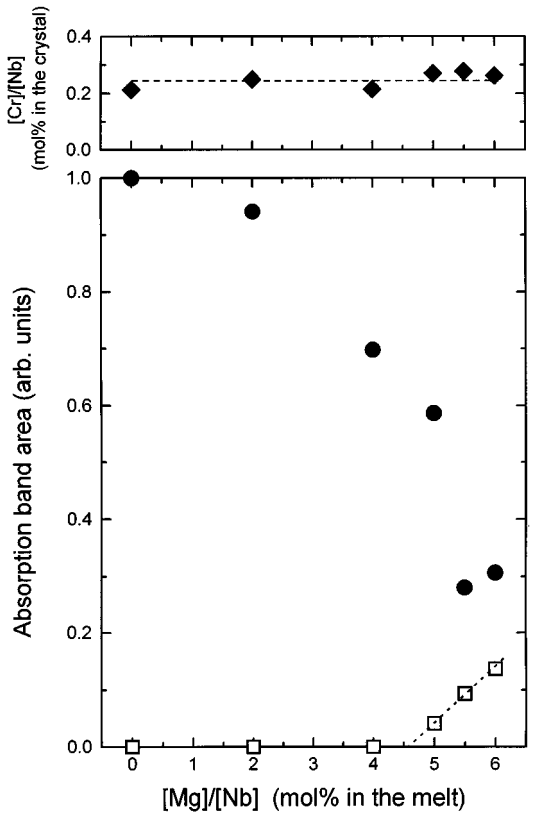

FIG. 2. Variation of the 530 nm (□) and 654 nm (●) broadband areas (see Fig. 1) as a function of the Mg content in the melt. In the upper part of the figure appears the chromium concentration incorporated to the crystals.

valence state are formed. Unfortunately no new optical absorption and EPR bands were observed in samples with Mg^{2+} ions concentration between 0 and 4%.

Let us consider again the optical absorption spectra presented in Fig. 1(a). The two broadbands and the narrow lines observed in Mg undoped $LiNbO_3$:Cr ($S0$) crystal were previously attributed to Cr^{3+} ions located at the Nb^{5+} site (Cr^{3+}_{Nb}).[3] More recently, the Cr^{3+} optical spectrum was tentatively ascribed to both Cr^{3+} in Li^+ and Nb^{5+} sites (Cr^{3+}_{Li} and Cr^{3+}_{Nb}). In contrast to the explanation based upon the coexistence of both centers, the $LiNbO_3$:Cr EPR spectrum was explained considering a unique Cr^{3+} center related to Cr^{3+} ions substituting for Li^+ sites.[10] This discrepancy between optical and EPR data was later explained by considering that most Cr ions were forming Cr^{3+}_{Li}-Cr^{3+}_{Nb} pairs, so that they could not be detected by EPR.[6] On the other hand, in heavily Mg codoped samples two EPR spectra coexist and have been attributed to Cr^{3+} ions substituting for the Li^+ site (Cr^{3+}_{Li}) and for the Nb^{5+} site (Cr^{3+}_{Nb}).[10,11] With the aim of correlating the EPR spectra due to these Cr^{3+} centers with the above-mentioned absorption bands, EPR measurements have been carried out for all crystals.

Figure 3 shows the room temperature EPR spectra of Cr^{3+} recorded with the magnetic field perpendicular to the c axis in two samples of $LiNbO_3$ with 2% and 6% Mg, respectively. The spectrum of the 2% Mg-doped crystal shows the lines arising from the well-known Cr^{3+} axial center, having a gyromagnetic factor $g \simeq 1.97$ and a zero-field-

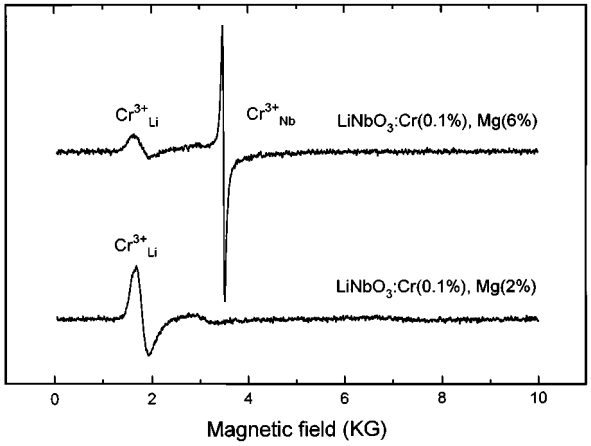

FIG. 3. EPR spectra of the $S2$ and $S6$ samples measured at room temperature with the magnetic field perpendicular to the crystal c axis.

splitting parameter $D \simeq 0.4$ cm^{-1}.[7–10] This spectrum, which is correlated with Cr^{3+}_{Li} centers, has been observed in all samples (from 0 to 6% doping levels), although its relative intensity varies with the Mg content, as will be described in what follows. On the other hand, for the 6% Mg sample one additional spectrum is observed. This new spectrum is also detected in the 5% and 5.5% Mg-doped crystals and consists of a single isotropic line appearing around 3500 G. This EPR spectrum was recently observed in $LiNbO_3$ heavily codoped with Mg and unambiguously attributed to Cr^{3+} substituting for Nb^{5+}, having $D \simeq 0$ cm^{-1}, by means of the ENDOR technique.[10,11]

Figure 4 shows the evolution of the intensity of the EPR signals due to Cr^{3+}_{Li} and Cr^{3+}_{Nb} centers as a function of the Mg concentration. The experimental points have been obtained from the area under the absorption curve of the low-field line (Cr^{3+}_{Li} center) and the isotropic line (Cr^{3+}_{Nb} center). In all cases the data were corrected for slight changes in the sample volume and quality factor Q of the cavity. A similar evolution was observed for the different lines in the axial spectrum as well as for magnetic field orientations other than $\mathbf{H} \perp c$.

The integrated EPR intensity of the axial center (Cr^{3+}_{Li}) shows a similar behavior to that observed for the area of the optical broadband centered at 654 nm [see Fig. 1(a)]. The inset in Fig. 4 shows a linear relation between the two integrated areas. On the basis of these experimental results we can conclude that the absorption broadbands at 487 and 654 nm are only due to Cr^{3+} in the Li^+ site (Cr^{3+}_{Li}).

A similar correspondence between the broadbands centered at 530 and 745 nm and the EPR isotropic line was observed. This indicates that the later new broadbands, which appeared for Mg concentration greater than 4%, are associated to Cr^{3+} ions in the Nb^{5+} site (Cr^{3+}_{Nb}).

Recently, the same assignment as in this work was published by Macfarlane *et al.*, where several centers of Cr^{3+} in the Li^+ site and Nb^{5+} site have been reported in two samples [$LiNbO_3$:Cr(0.1%) and $LiNbO_3$:Cr(0.1%),Mg(6%)] using fluorescence line narrowing.[18]

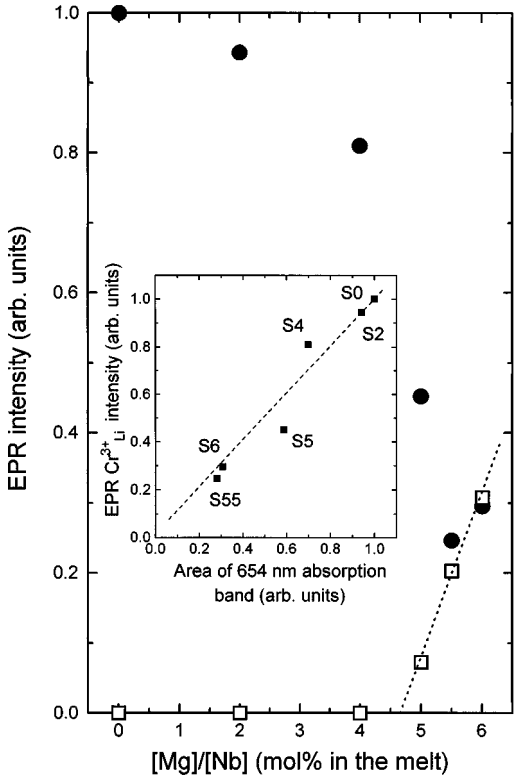

FIG. 4. Evolution of the area under the EPR absorption curve associated with Cr^{3+} in the Li site (●) and Cr^{3+} in the Nb site (□) with Mg concentration. The inset shows the close linear relationship between the area of the EPR spectrum and the 654 nm absorption broadband.

The above assignment of the broadband spectra of Cr^{3+} can be helpful to understand the observed changes in the near-ultraviolet (UV) absorption region of $LiNbO_3$:Cr and $LiNbO_3$:Cr,Mg crystals [see Fig. 1(a)]. For pure congruent crystals of $LiNbO_3$ it is known that the absorption edge lies at 320 nm,[19] while this absorption edge appears slightly shifted to shorter wavelengths for doped $LiNbO_3$:Mg crystals.[20] However, as can be observed in the inset of Fig. 5, a strong absorption rise appears departing from around 400 nm in chromium-doped samples.

In order to investigate the evolution of this absorption rise with the Mg concentration, we identify it as the wavelength Δ corresponding to an absorption coefficient value of 15 cm^{-1}. Figure 5 shows Δ as a function of the Mg concentration. For Mg doping levels between 0 and 4%, Δ shifts to shorter wavelengths while for Mg content greater than 4%, Δ turns abruptly back to longer wavelengths. The extrapolated fitting shows again a threshold for a Mg concentration of 4.6%. Therefore the UV absorption edge in Mg-doped $LiNbO_3$ crystals follows the same trend observed for the Cr^{3+}_{Li} sites in the 0 to approximately 4.6% Mg doping range and for the Cr^{3+}_{Nb} center over this threshold.

The Mg^{2+} threshold value (4.6%) found in this work for the appearance of Cr^{3+} in Nb^{5+} sites as well as the abrupt shifting in the UV absorption region, coincides with the Mg doping level which produces strong changes in many properties of $LiNbO_3$, for instance, the reduction of the optical damage,[12] the creation of oxygen vacancies in reduced

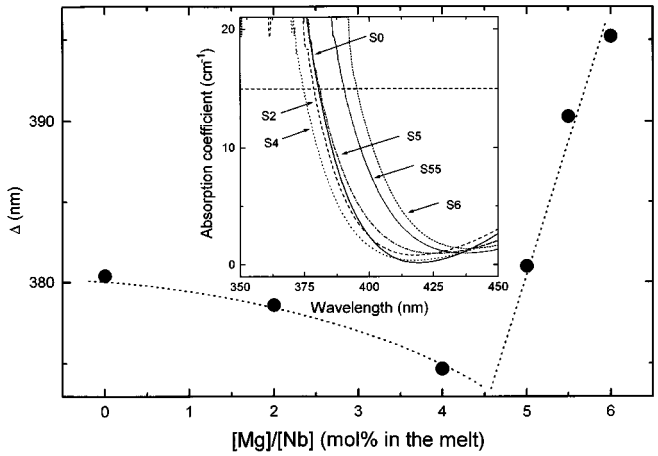

FIG. 5. Wavelength value Δ corresponding to an absorption coefficient value of 15 cm^{-1} as a function of the Mg concentration. The inset shows the absorption spectra of *S*0, *S*2, *S*4, *S*5, *S*55, and *S*6 crystals measured at room temperature in the near-UV range.

$LiNbO_3$:Cr,Mg crystals,[21] and the variation of the infrared absorption bands due to the O-H bond stretching vibration.[22]

This threshold of 4.6% can be discussed considering the two cation substitution models reported in the literature for the nonstoichiometry phenomena of $LiNbO_3$. In both models the Li^+ deficiency leads to the occupation of some percentage of Li^+ sites by Nb^{5+} ions, the so-called Nb antisites. However, the mechanisms for total charge compensation are different. The Li-site vacancy model is expressed by the chemical formula $[Li_{1-5x}Nb_x\square_{4x}][Nb]O_3$, where the first square brackets express the ions located at Li site and the second ones the ions located at the Nb site. Nb_x denotes the antisite (Nb substituting for Li) concentration and $\square_{4x}$ the Li-site vacancy concentration.[23,24] The Nb-site vacancy model is related to the formula $[Li_{1-5x}Nb_{5x}][Nb_{1-4x}\square_{4x}]O_3$, where Nb_{5x} represents the antisite concentration and $\square_{4x}$ the Nb-site vacancy concentration.[25,26] For congruent $LiNbO_3$ materials the [Li]/[Nb] ratio is 94.5%.[27] Considering this ratio, both models give for x the same value $x=0.009$. Using this data in the Li-site vacancy model the calculated antisite concentration and Li-site vacancies are 0.9% and 3.7%, respectively. For the Nb-site vacancy model concentrations of 4.6% and 3.7% for the antisites and Nb-site vacancies are, respectively, found. According to Watanabe *et al.*,[28] we assume that Mg ions are incorporated into Li sites (Li-site vacancies as well as antisites). Thus a total amount of 4.6% available sites for the Mg ions is obtained in both models for congruent crystals (as those used in this work). This value coincides with that found in the present work for the threshold observed in the appearance of the Cr^{3+}_{Nb} centers.

Accepting now that Cr^{3+}_{Li} centers correspond to chromium ions that are incorporated in both antisites and Li-site vacancies, it would be expected that the amount of Cr^{3+} in Li^+ sites should be reduced in Mg-doped samples. In fact Mg^{2+} tends to replace Nb^{5+} antisites (or the associated Li^+ vacancies in the Li-site vacancy model), leaving less available Li^+ sites for the Cr^{3+} ions. This explains the changes observed in the Cr^{3+} ion distribution by only codoping with a few percent ($\leqslant$6%) of MgO. In addition, accord-

ing to both models, for Mg doping levels higher than 4.6%, all available sites for the Mg^{2+} ions (Nb^{5+} antisites and Li^{+} vacancies) should be filled preferentially by Mg^{2+} ions. Thus some Cr^{3+} ions should be obliged to occupy other cation sites. This would explain the appearance of Cr_{Nb}^{3+} sites over this Mg threshold level of 4.6%.

It is clear that the above considerations ignore the changes induced in the [Li]/[Nb] ratio by the Mg^{2+} ions incorporation in the crystals, an aspect that should be included in a more reliable explanation.

IV. CONCLUSION

Optical absorption and electron spin resonance measurements taken on $LiNbO_3$:Cr and $LiNbO_3$:Cr,MgO crystals reveal an interplay between Cr_{Li}^{3+} and Cr_{Nb}^{3+} ions. For codoped samples below 4.6% of MgO all Cr^{3+} ions lie at Li^{+} sites. Above this Mg threshold a percentage of Cr^{3+} ions is displaced to occupy Nb^{5+} sites. The relative concentration of both Cr^{3+} centers produces a significant change in the color of the crystals and provides the possibility of color control by MgO codoping.

*Electronic address: fjaque@vm1.sdi.uam.es

[1] A. Córdova-Plaza, M. Digonnet, and H. J. Shaw, IEEE J. Quantum Electron. **QE-23**, 26 (1987).
[2] Y. Qiu, J. Phys. Condens. Matter **5**, 2041 (1993).
[3] A. M. Glass, J. Chem. Phys. **50**, 1501 (1969).
[4] J. Weiyi, L. Huimin, R. Knutson, and W. M. Yen, Phys. Rev. B **41**, 10 906 (1989).
[5] E. Camarillo, J. Tocho, I. Vergara, E. Díeguez, J. García Solé, and F. Jaque, Phys. Rev. B **45**, 4600 (1992).
[6] F. Jaque, J. García-Solé, E. Camarillo, F. J. López, H. Murrieta, and J. M. Hernández, Phys. Rev. B **47**, 5432 (1993).
[7] G. Burns, D. F. O'Kane, and R. S. Title, Phys. Lett. **23**, 56 (1967).
[8] D. G. Rexford, Y. M. Kim, and H. S. Story, J. Chem. Phys. **52**, 860 (1970).
[9] G. I. Malovichko, V. G. Grachev, and S. N. Lukin, Sov. Phys. Solid State **28**, 553 (1986).
[10] A. Martín, F. J. López, and F. Agulló-López, J. Phys. Condens. Matter **5**, 6221 (1992).
[11] G. Corradi, H. Söthe, J. M. Spaeth, and K. Polgár, J. Phys. Condens. Matter **3**, 1901 (1991).
[12] A. G. Zhong, J. Jin, and W. Zhong-Kang, Proceedings of the 11th International Quantum Electronics Conference, Institute of Electrical and Electronic Engineers, IEEE Cat. No. 80 CH 1561 (IEEE, New York, 1980).
[13] A. Lorenzo, H. Jaffrezic, B. Roux, G. Boulon, and J. García Solé, Appl. Phys. Lett. **67**, 1 (1995).
[14] A. Prange, Spectrochim. Acta **B44**, 437 (1989).
[15] K. Nassau, in *Ferroelectricity*, edited by E. F. Weller (Elsevier, Amsterdam, 1967).
[16] K. Feisst and A. Räuber, J. Cryst. Growth **63**, 337 (1983).
[17] A. Abragam and B. Bleaney, *Electron Paramagnetic Resonance of Transition Ions* (Clarendon, Oxford, 1970).
[18] P. I. Macfarlane, K. Holliday, J. F. H. Nicholls, and B. Henderson, J. Phys. Condens. Matter **7**, 9643 (1995).
[19] I. Földvari, K. Polgár, R. Vozska, and R. N. Balasanyang, Cryst. Res. Technol. **19**, 1659 (1984).
[20] K. Polgár, L. Kovács, I. Földvári, and I. Cravero, Solid State Commun. **59**, 375 (1986).
[21] K. L. Sweeney, L. E. Halliburton, D. A. Bryan, R. R. Rice, R. Gerson, and H. E. Tomaschke, Appl. Phys. Lett. **45**, 805 (1984).
[22] D. A. Bryan, R. R. Rice, R. Gerson, H. E. Tomaschke, K. L. Sweeney, and L. E. Halliburton, Opt. Eng. **24**, 143 (1985).
[23] P. Lerner, C. Legras, and J. P. Dumas, J. Cryst. Growth **3-4**, 231 (1968).
[24] N. Iyi, K. Kitamura, F. Izumi, J. K. Yamamoto, T. Hayashi, H. Asano, and S. Kimura, J. Solid State Chem. **101**, 340 (1992).
[25] G. E. Peterson and A. Carnevale, J. Chem. Phys. **56**, 4848 (1972).
[26] S. C. Abrahams and P. Marsh, Acta Crystallogr. B **42**, 61 (1986).
[27] J. R. Carruthers, G. E. Peterson, M. Grasso, and P. M. Bridenbaugh, J. Appl. Phys. **42**, 1846 (1971).
[28] Y. Watanabe, T. Sota, K. Suzuki, N. Iyi, K. Kitamura, and S. Kimura, J. Phys. Condens. Matter **7**, 3627 (1995).